PATH GENERATION ANALYSIS OF FLEXIBLE MANIPULATORS

A Thesis Submitted to
the Graduate School of Engineering and Sciences of
İzmir Institute of Technology
in Partial Fulfillment of the Requirements for the Degree of

MASTER OF SCIENCE

in Mechanical Engineering

by
Hakan BİNGÖL

October 2008
İZMİR

We approve the thesis of **Hakan BİNGÖL**

Assist. Prof. Dr. Ebubekir ATAN

Supervisor

Prof. Dr. Ramazan KARAKUZU

Committee Member

Assoc. Prof. Dr. Bülent YARDIMOĞLU

Committee Member

Assist. Prof. Dr. Ebubekir ATAN

Committee Member

---

16 October 2008

Assoc. Prof. Dr. Metin TANOĞLU

Head of the Mechanical Engineering Department

Prof. Dr. Hasan BÖKE

Dean of the Graduate School of Engineering and Sciences

ACKNOWLEDGEMENTS

I wish to express my sincere gratitude to my advisors Assist. Prof. Dr. Ebubekir ATAN his supervisions, guidance, encouragement and supports during the courses of this thesis and in the experimental study.

I would like to thank to Committee Members Prof. Dr. Ramazan KARAKUZU and Assoc. Prof. Dr. Bülent YARDIMOĞLU for their comments and suggestions during my thesis.

Finally, I would like to thank my family, and my friend Evrim ÖZDAMAR especially for their understanding, encouragement and supports.

ABSTRACT

PATH GENERATION ANALYSIS OF FLEXIBLE MANIPULATORS

By the improving technology, usage of robotic manipulators has been increased a lot in last decades. Robotic manipulators are usually used in continuous production and dangerous operations. General industries, medical applications and space missions are the most important usage areas for these manipulators. In these applications, the manipulator faces to deviation of the end effecter which depends on many reasons like friction, vibration, elastic and plastic deformations. However, the robotic calculations made, as the links of the manipulator are rigid and other effects are neglected.

The aim of this thesis is to improve a path generation analysis method for the three link flexible planer manipulator. The three link manipulator is considered to investigate the flexibility effect of links on path generation. Firstly the problem and solution method is introduced then the inverse kinematic analysis is applied for the three link rigid planer manipulator. The finite element model of the three link flexible planer manipulator is developed by using the plane frame element. The general equations of the tip point displacements of the three link flexible planer manipulator are expressed and Matlab® program is coded. Finally, the library robots made by aluminum and steel are chosen for numerical examples. In conclusion the results of numerical example are shown for each position of the manipulator and discussed.

ÖZET

ESNEK MANİPULATÖRLERİN YÖRÜNGE OLUŞTURMA ANALİZİ

Gelişen teknoloji ile robot kollar, sanayi başta olmak üzere birçok alanda kullanılmaktadır. Bir robot kolunun çalışmasında en önemli ve istenilen özellik, analitik olarak hesaplanan denklemler sonucu robot uç işlevcisinin istenilen konuma en az hatayla ulaşmasıdır. Bazı nedenlerden dolayı; sürtünme, titreşim, uzuvlarda oluşan esnek ve kalıcı deformasyonlar vs. robot uç işlevcisinin matematiksel olarak hesaplanan noktaya ulaşması mümkün olmamaktadır.

Bu tezinin amacı, esnek üç uzuvlu düzlemsel bir robot kolunun çalışması sırasında robot kolunun uç noktasında oluşan elastik deformasyonların, tasarlanan bir kütüphane robotu üzerinde sonlu eleman analizi yaparak hesaplamaktır. Öncelikle problem ve problemin çözümünde uygulanacak yöntem anlatılmıştır. Ardından ters kinematik analiz yöntemi ile robotun açısal konumu için genel formüller bulunmuş ve sonlu eleman analizi için düzlemsel birim sonlu eleman tanıtılmıştır; Sonlu eleman analizinde kullanılacak formüller Matlab® programında bulunmuş ve analiz yönteminin esnek üç uzuvlu düzlemsel robota nasıl uygulanacağı açıklanmıştır. Ardından bulunan genel formüllerde kullanılacak sayısal değerler için analiz yapılmış, kütüphane robotunun malzeme özellikleri ve boyutları gösterilmiştir. Son olarak verilen değerler için robot uç işlevcisinin tanımlanan yörüngelerdeki yatay ve dikey yer değiştirmeleri gösterilmiş ve yorumlanmıştır.

TABLE OF CONTENTS

LIST OF FIGURES

Figure **Page**

LIST OF TABLES

Table **Page**

CHAPTER 1

INTRODUCTION

By the improving technology, usage of robotic manipulators has been increased a lot in the last decades. Robotic manipulators are usually used in speed required and dangerous operations. General industries, medical applications and space missions are the most common usage areas for the manipulators. In these applications, link flexibility is usually neglected so the manipulator faces to deviation of the end effecter. This problem causes the production failures and faulty operations. On the other hand, the power costs of the rigid manipulators are higher then the flexible ones which consume less power due to having lighter link masses than the rigid and bulky manipulators. Also the faster movements can be achieved with this kind of manipulators. In addition, these manipulators are especially suitable for a number of non-conventional robotic applications, including space missions. All these advantages make the study of flexible robot manipulators quite interesting. So it is no longer possible to assume that link deformation can be neglected.

During the past two decades, there has been an increasing interest in kinematic and dynamic formulation of flexible manipulators. For modeling a flexible robot manipulator by using combined Lagrange-Assumed Modes Approach; (Book, 1984), (De Luca and Siciliano, 1991), (Yuan *et al,* 1993), (Canudas de Wit *et al,* 1996), derived the equations in a closed form. With flexible manipulators it is understood that there's not an independent control input for each degree of freedom.(De Luca and Siciliano, 1993) ,(De Luca and Panzieri, 1994) found some results for point to point analysis of flexible manipulators. The condition of neglecting modal damping of the links is treated by making some assumptions on the inertia matrix is showed by in (Deluca and Siciliano, 1993). In 1994 Deluca and Panzieri improved a method for the situation of unknown gravity vector. To increase the damping of the system (Dawson, 1991) assumed the no damping case.

It is easily understood that modeling of a flexible manipulators is a challenging task. Since the nominal or rigid body motion changes the geometry of the system, the system parameters vary with time and subsequently influence the elastic deformations of the interconnected bodies. On the other hand, the elastic deformations influence the

rigid link kinematics of the interconnected system. This is why the flexible manipulator's dynamic equations involve highly complex equations. The dynamic formulation of flexible multibody systems leads to a set of complicated partial differential equations; these equations are space and time dependent so they can not be solved analytically.

In this thesis, three links manipulator is considered to investigate the flexibility effect of links on path generation. Chapter 2 is given to introduce the problem and solution method. Chapter 3 deals with the inverse kinematic analysis of three links rigid planer manipulator. Chapter 4 introduces plane frame finite element. Chapter 5 presents finite element model of the three links flexible planer manipulator. Chapter 6 discusses the results of the numerical examples results and conclusion is given in chapter 7.

CHAPTER 2

PROBLEM DESCRIPTION&METHOD

2.1. Statement of the Problem

There are several effects to avoid reaching the gripper desired position. These are static forces, stiffness (link flexibility), gravity, joint flexibility, damping, Coriolis acceleration and so on. Some of them take in to account but others usually neglected in literature because of the simplification of the equations.

In this thesis, it is desired to find the total deflection of the tip. A planer manipulator with three revolute joints and links is defined in a planer path as if a library robot. It is shown in Figure 2.1.

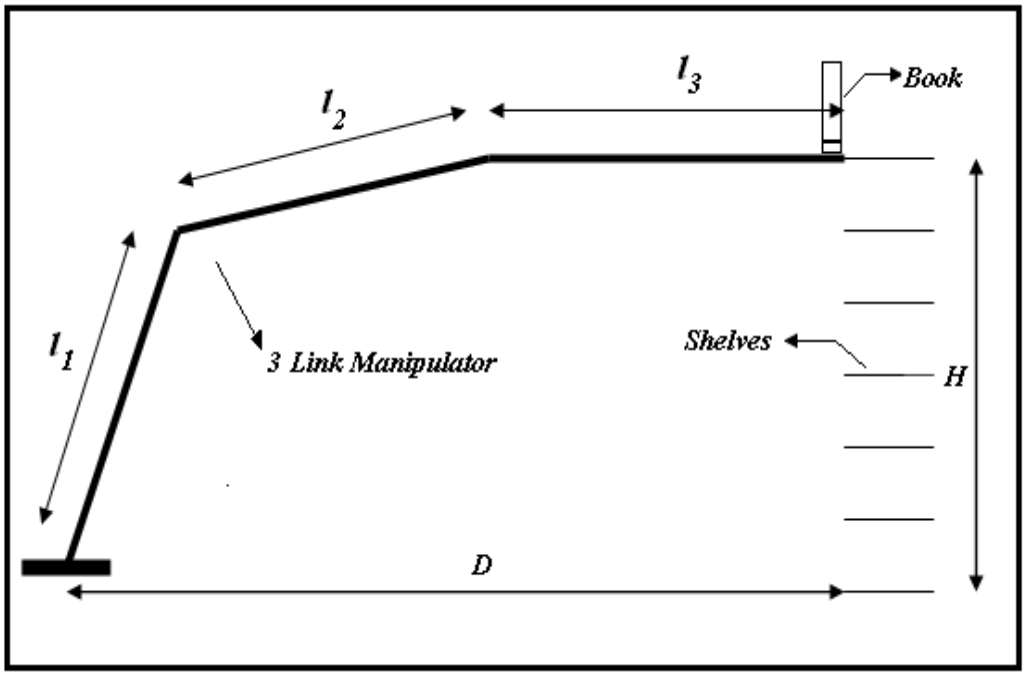

Figure 2.1. The planer manipulator with three revolute joints

Firstly, three links manipulator assumed to be rigid and the points that the gripper reaches are found. Furthermore, the links flexibility has been taken into account

and the displacements have found for the flexible planer manipulator with finite element analysis.

2.2. Solution Method

The tip displacements of the three links planer flexible manipulator are solved by applying the joint angles in global coordinate system, driven from the inverse kinematic analysis. The general equations of joint angles are found by the developed algorithm with Matlab. For the finite element analysis of three links planer manipulator, the plane frame element is defined in global coordinate system. By using the plane frame element, the general finite element model of the three links flexible planer manipulator is designed. With the developed program in Matlab, general equations for the displacements of the tip point of the three links planer flexible manipulator are found and the formulation is applied on given numerical example of a considered library robot. In conclusion, the results of numerical examples are found and discussed. For all examples the factor of safety is considered about "4" and the strength analysis for the manipulators has done for each position.

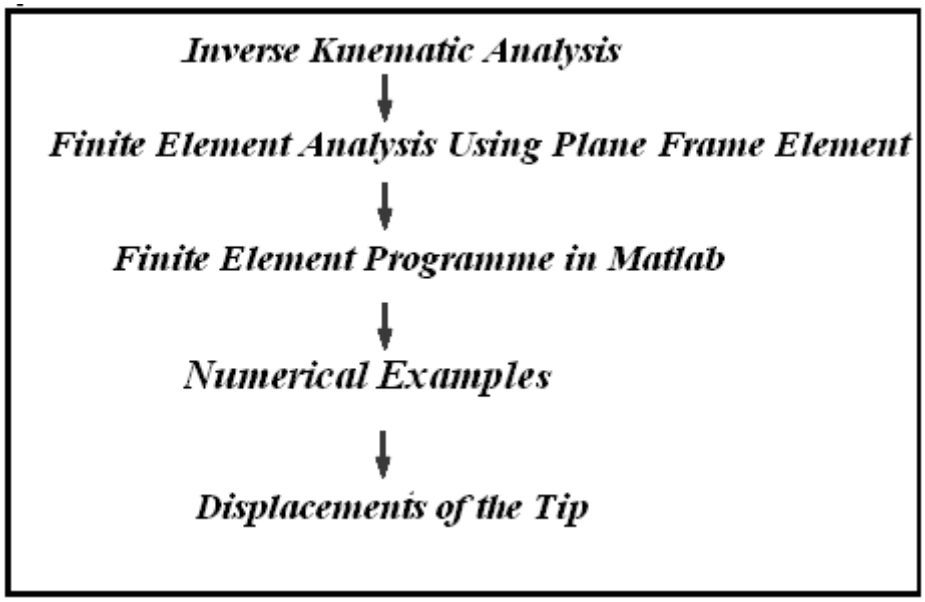

Figure 2.2. Solution method

CHAPTER 3

KINEMATIC ANALYSIS OF THREE LINKS RIGID PLANER MANIPULATOR

3.1. **Fundamentals**

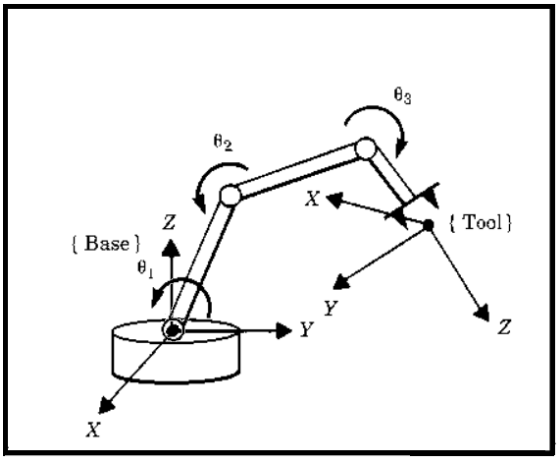

Figure 3.1. The three link manipulator
(Source: Craig 1989)

In Figure 3.1, the three link manipulator is shown. The links are connected with each other by joints. The angles between links are called joint angles. In robotic applications usually the joints have motors to provide the joint angles which will give desired position of the tip and each joint has sensors to control joint angles. In general, manipulators have revolute joints and prismatic joints. In this thesis, path generation of the planer manipulator is investigated.

3.2. **Inverse Kinematic Analysis**

The joints angles are found by calculations backward from tip point to the base of the robot with inverse kinematic analysis for the desired position of the tip point. In inverse kinematic analysis, the analytical formulations are used to calculate the angles between the joints.

This analysis is important because desired position of the tip point must be in reachable point in work space and the desired orientation of the links must be defined in considered coordinate frame. If one of these conditions is not verified, there is no solution exists for the inverse kinematic analysis. On the other hand to find the angles of the manipulator for each position, there is more than one solution. In Figure 3.2, the way to reach the tip point desired position; it can be easily seen that there are two possible configurations. So it is important that which solution is suitable for the desired work of the manipulator.

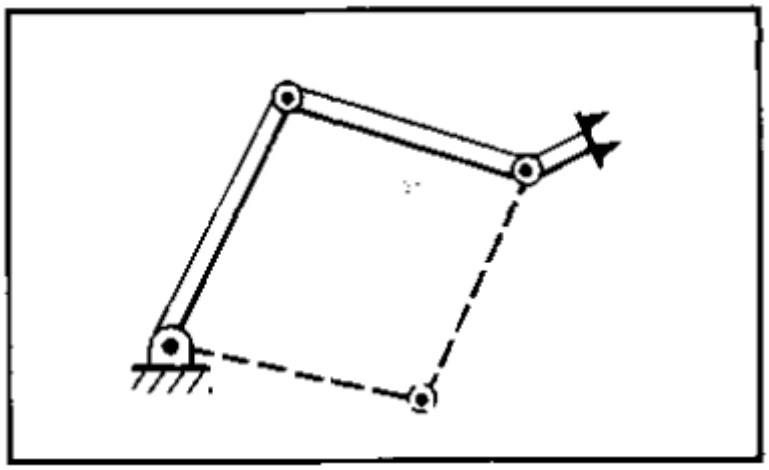

Figure 3.2. Multiple solutions
(Source: Craig 1989)

3.2.1. **Algebraic Method**

In Figure 3.3, three link rigid planer manipulator is shown. Transformation matrix from base to griper is written as;

$$ {}^{B}_{G}T = \begin{bmatrix} c\phi & -s\phi & 0 & x \\ s\phi & c\phi & 0 & y \\ 0 & 0 & 1 & 0 \\ 0 & 0 & 0 & 1 \end{bmatrix} \tag{2.1} $$

To find the angles of the links for desired position of the tip point, the inverse kinematic analysis task should be applied.

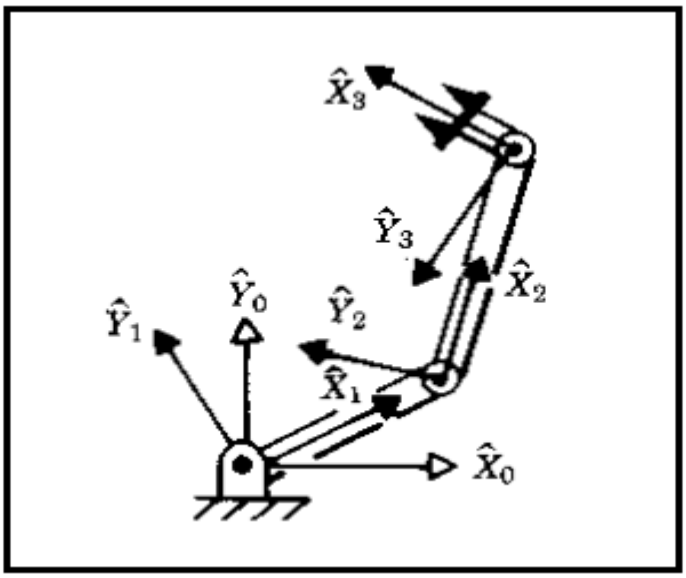

Figure 3.3. The three link rigid manipulator
(Source: Craig 1989)

The angle "ϕ" is dependents on "$\theta_1, \theta_2, \theta_3$"

$$X = l_1.c_1 + l_2.c_{12} \tag{2.2}$$

$$Y = l_1.s_1 + l_2.s_{12} \tag{2.3}$$

$$X^2 + Y^2 = l_1^2 + l_2^2 + 2l_1.l_2.c_2 \tag{2.4}$$

$$c_2 = \frac{X^2 + Y^2 - l_1^2 - l_2^2}{2l_1.l_2} \tag{2.5}$$

Assuming that the desired position is in workspace;

$$s_2 = \pm\sqrt{1 - c_2^2} \tag{2.6}$$

"θ_2" is found using two argument arctangent routine;

$$\theta_2 = A\tan 2(s_2, c_2) \tag{2.7}$$

The choice of signs corresponds to the multiple solutions in which the elbow of the manipulator is up or down. After finding "θ_2", "θ_1" is found.

$$X = k_1.c_1 - k_2.s_1 \tag{2.8}$$

$$Y = k_1.s + k_2.c_1 \tag{2.9}$$

Where;

$$k_1 = l_1 + l_2.c_2 \tag{2.10}$$

$$k_2 = l_2.s_2 \tag{2.11}$$

For solving these equations, there are some variables defined;

$$r = \pm\sqrt{k_1^2 + k_2^2} \tag{2.12}$$

$$\gamma = A\tan 2(k_2, k_1) \tag{2.13}$$

$$k_1 = r.\cos\gamma \tag{2.14}$$

$$k_2 = r.\sin\gamma \tag{2.15}$$

From these equations;

$$\frac{x}{r} = \cos\gamma.\cos\theta_1 - \sin\gamma.\sin\theta_1 = Cos(\theta_1 + \gamma) \tag{2.16}$$

$$\frac{y}{r} = \cos\gamma.\sin\theta_1 + \sin\gamma.\cos\theta_1 = Sin(\theta_1 + \gamma) \tag{2.17}$$

$$\gamma + \theta_1 = A\tan 2(\frac{y}{r}, \frac{x}{r}) = A\tan 2(y, x) \tag{2.18}$$

$$\theta_1 = A\tan 2(y, x) - A\tan 2(k_2 - k_1) \tag{2.19}$$

Finally "θ_3" is found from known "θ_1, θ_2, ϕ" angles,

$$\theta_1 + \theta_2 + \theta_3 = A\tan 2(s\phi, c\phi) = \phi \tag{2.20}$$

3.2.2. **Geometric Method**

To find the joint angles of three links planer manipulator with geometric method, the equations are derived from the simple geometry. As it seen in Figure 3.4, there are two possible way to reach the tip point of the griper desired position. The dashed lines show the other possible way to reach the griper desired point.

$$\alpha = \tan^{-1}\left(\frac{r_y}{r_x}\right) \tag{2.21}$$

$$(l_1)^2 + (l_2)^2 - 2.l_1.l_2.\cos 2\beta = (r_x)^2 + (r_y)^2 \tag{2.22}$$

$$2\beta = \cos^{-1}\left(-\frac{(r_x)^2 + (r_y)^2 - (l_1)^2 - (l_2)^2}{2.l_1.l_2}\right) \tag{2.23}$$

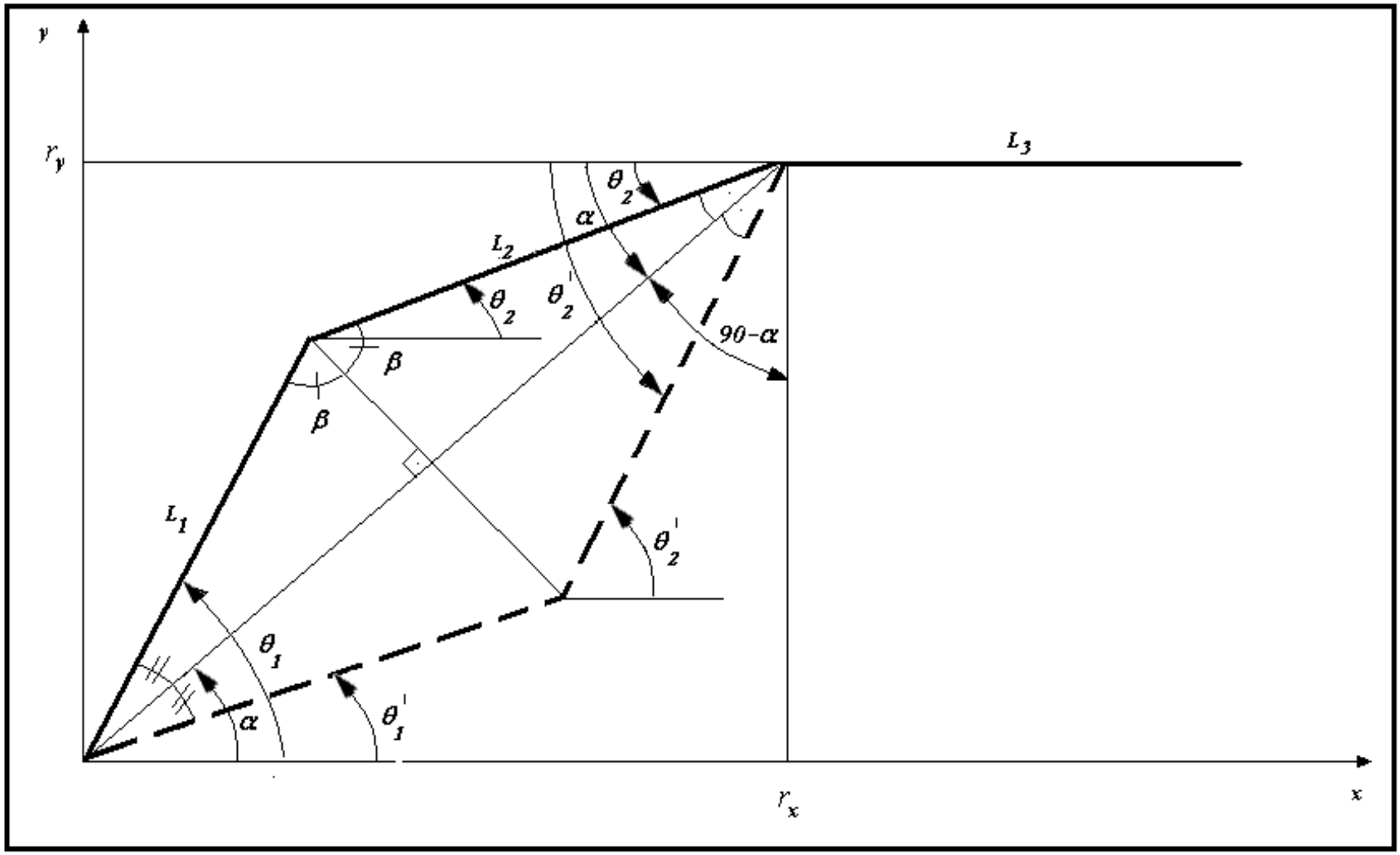

Figure 3.4. A plane geometry of the three link planer manipulator

"θ "values can be easily calculated for each solution as follows;

For the First Solution:

$$\theta_1 = \alpha + (90 - \beta) \tag{2.24}$$

$$\theta_2 = 90 - (90 - \alpha) - (90 - \beta) = \alpha + \beta - 90 \tag{2.25}$$

For the Second Solution:

$$\theta_1' = \alpha - (90 - \beta) \tag{2.26}$$

$$\theta_2' = \alpha + (90 - \beta) \tag{2.27}$$

CHAPTER 4

PLANE FRAME FINITE ELEMET

4.1. Defining Element

This chapter deals with the frame element for finite element analysis. For this analysis a straight bar with arbitrary cross section is selected. The bar is capable of carrying axial forces, transverse forces and moments. This element can deform in axial direction and direction perpendicular to the axis of the bar. The used frame element is shown in Figure 4.1.

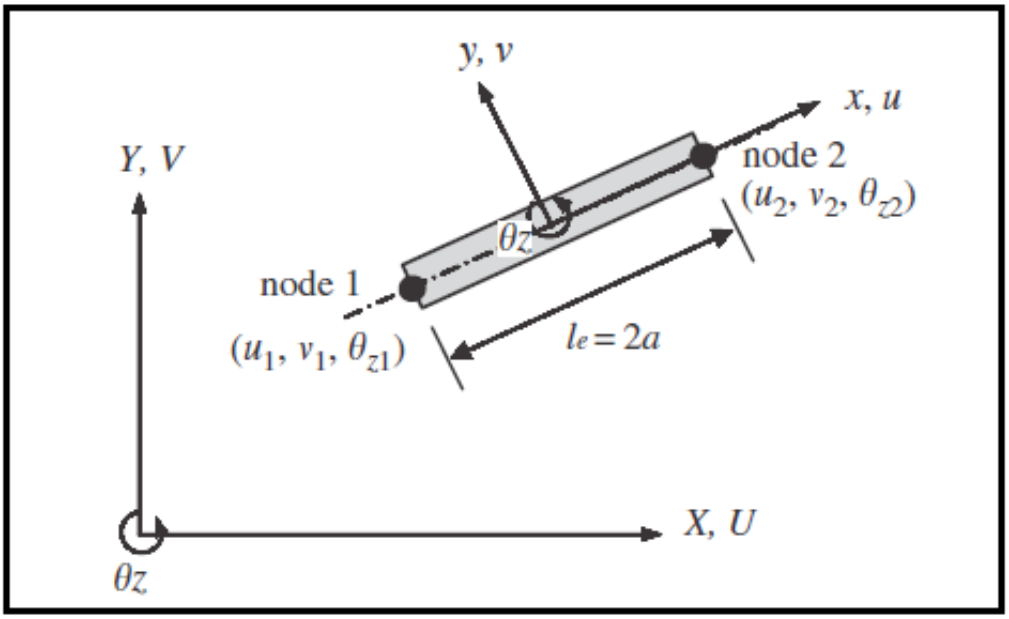

Figure 4.1. Frame element of the link

(Source: Liu 1993)

4.2. Finite Element Equations in Local Coordinate System

The frame structure consists of frame elements which are connected by nodes. Element length is considered “2a” and each element has two nodes at its tips.

The planar frame element has 3 degrees of freedom at one node in its local coordinate system, as shown in Figure 4.1.

Where;

U; Axial deformation in the "x" direction,

V; Deflection in the "y" direction,

θ_Z ; Rotation in the "x–y" plane and with respect to the "z"-axis,

So, each element is defined with two nodes has a total of 6 degrees of freedoms. (Liu, 1993)

The frame element has both the properties of the truss element and the beam element. The element matrices for a frame element can be calculated by combining element matrices for truss and beam elements. The truss element has only one degree of freedom at each node (axial deformation), and the beam element has two degrees of freedom at each node (transverse deformation and rotation). Combining these knowledge give the degrees of freedom and displacements of a frame element in Equation 4.1 (Liu, 1993)

$$d_e = \begin{Bmatrix} d_1 \\ d_2 \\ d_3 \\ d_4 \\ d_5 \\ d_6 \end{Bmatrix} = \begin{Bmatrix} U_1 \\ V_1 \\ \theta_{Z1} \\ U_2 \\ V_2 \\ \theta_{Z2} \end{Bmatrix} \tag{4.1}$$

The stiffness matrix "k_e" for truss element is shown in Equation 4.2;

$$k_e^{truss} = \begin{bmatrix} AE/(2a) & 0 & 0 & -AE/(2a) & 0 & 0 \\ & 0 & 0 & 0 & 0 & 0 \\ & & 0 & 0 & 0 & 0 \\ & & & AE/(2a) & 0 & 0 \\ & sy. & & & 0 & 0 \\ & & & & & 0 \end{bmatrix} \tag{4.2}$$

The stiffness matrix "k_e" for beam element is shown in Equation 4.3;

$$k_e^{beam} = \begin{bmatrix} 0 & 0 & 0 & 0 & 0 & 0 \\ & \frac{3EI_z}{2a^3} & \frac{3EI_z}{2a^2} & 0 & -\frac{3EI_z}{2a^3} & \frac{3EI_z}{2a^2} \\ & & \frac{2EI_z}{a} & 0 & -\frac{3EI_z}{2a^2} & \frac{EI_z}{a} \\ & & & 0 & 0 & 0 \\ & sy. & & & \frac{3EI_z}{2a^3} & -\frac{3EI_z}{2a^2} \\ & & & & & \frac{2EI_z}{a} \end{bmatrix} \tag{4.3}$$

To construct the stiffness matrix for frame element, stiffness matrix for truss element and beam element are extended to a "6×6" matrix corresponding to the order of the degrees of freedom of the truss element and beam element of the element displacement vector. The two matrices in Equation 4.2 and 4.3 are superimposed together to obtain the stiffness matrix for the frame element in Equation 4.4. (Liu, 1993)

$$k_e = \begin{bmatrix} \frac{AE}{2a} & 0 & 0 & -\frac{AE}{2a} & 0 & 0 \\ & \frac{3EI_z}{2a^3} & \frac{3EI_z}{2a^2} & 0 & -\frac{3EI_z}{2a^3} & \frac{3EI_z}{2a^2} \\ & & \frac{2EI_z}{a} & 0 & -\frac{3EI_z}{2a^2} & \frac{EI_z}{a} \\ & & & \frac{AE}{2a} & 0 & 0 \\ & sy. & & & \frac{3EI_z}{2a^3} & -\frac{3EI_z}{2a^2} \\ & & & & & \frac{2EI_z}{a} \end{bmatrix} \tag{4.4}$$

The same procedure can be applied to the force vector of frame element. If the element is loaded by external distributed forces "F_x" and "F_y" along the "x-axis"; concentrated forces "$F_{sx1}, F_{sx2}\ F_{sy1}, F_{sy2}$"; and concentrated moments "M_{s1}, M_{s2}" at node "1" and "2", the total nodal force vector becomes as it seen in Equation 4.5. (Liu, 1993)

$$f_e = \begin{Bmatrix} f_x a + f_{sx1} \\ f_y a + f_{sy1} \\ f_y a^2/3 + m_{s1} \\ f_x a + f_{sx2} \\ f_y a + f_{sy2} \\ -f_y a^2/3 + m_{s1} \end{Bmatrix} \tag{4.5}$$

4.3. **Finite Element Equations in Global Coordinate System**

The matrices calculated in Section 4.2 are in a specific orientation for particular frame element. A full frame structure usually consists of numerous frame elements of different orientations joined together. So, their local coordinate system would vary from

one orientation to another. To combine the element matrices together, all the matrices must be expressed in a common coordinate system, which is the global coordinate system. Assume that local nodes "1" and "2" correspond to the global nodes "i" and "j". The displacement at a local node should have two translational components in the "x" and "y" directions and one rotational deformation. They are numbered sequentially by "U", "V" and "θ_Z" at each of the two nodes, as shown in Figure 4.2. (Liu, 1993)

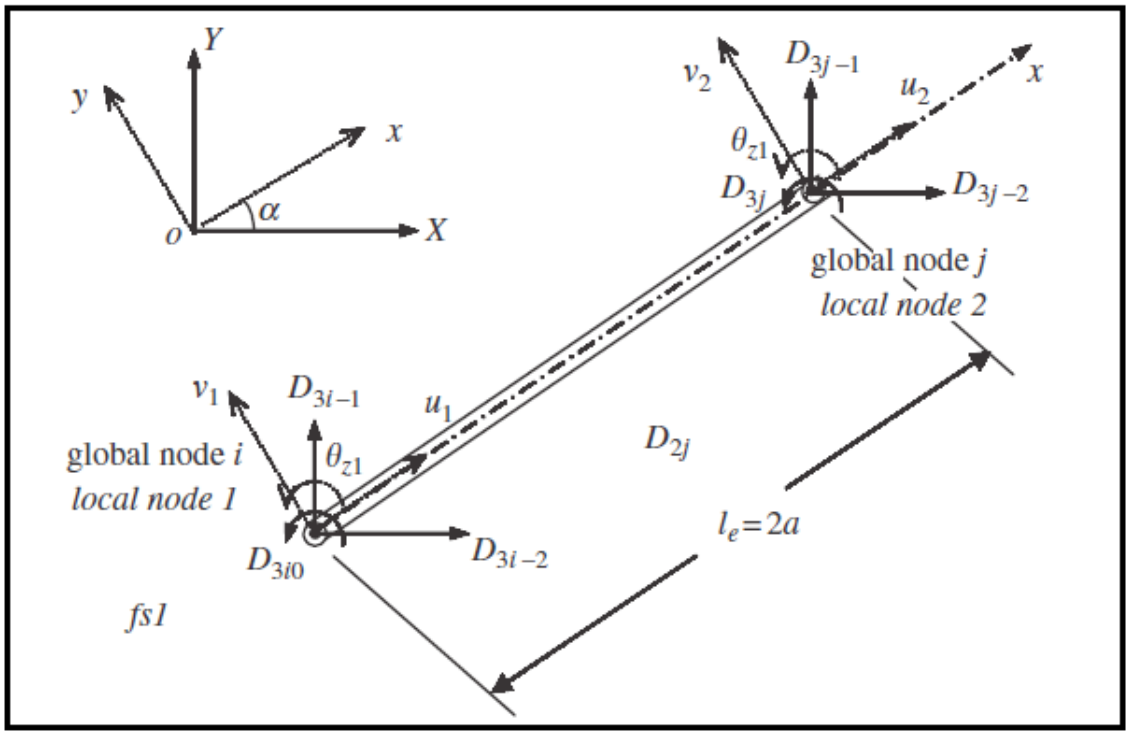

Figure 4.2. Frame element in global coordinates

(Source: Liu, 1993)

The displacement at a global node should also have two translational components in the "X" and "Y" directions and one rotational deformation. They are numbered sequentially by "D_{3i-2}", "D_{3i-1}" and "D_{3i}" for the "i" th node, as shown in Figure 4.2. The same sign convention also applies to node "j". The coordinate transformation gives the relationship between the displacement vector "d_e" based on the local coordinate system and the displacement vector "D_e" for the same element, but based on the global coordinate system.

$$d_e = T.D_e \tag{4.6}$$

$$D_e = \begin{Bmatrix} D_{3i-2} \\ D_{3i-1} \\ D_{3i} \\ D_{3j-2} \\ D_{3j-1} \\ 3j \end{Bmatrix} \tag{4.7}$$

"T" is the transformation matrix for the frame element is given by in Equation 4.8.

$$T = \begin{bmatrix} l_x & m_x & 0 & 0 & 0 & 0 \\ l_y & m_y & 0 & 0 & 0 & 0 \\ 0 & 0 & 1 & 0 & 0 & 0 \\ 0 & 0 & 0 & l_x & m_x & 0 \\ 0 & 0 & 0 & l_y & m_y & 0 \\ 0 & 0 & 0 & 0 & 0 & 1 \end{bmatrix} \tag{4.8}$$

In which;

$$l_x = \cos(x, X) = \cos\alpha = \frac{X_j - X_i}{l_e} \tag{4.9}$$

$$l_y = \cos(y, X) = \cos(90 + \alpha) = -\frac{Y_j - Y_i}{l_e} \tag{4.10}$$

$$m_x = \cos(x, X) = \sin\alpha = \frac{Y_j - Y_i}{l_e} \tag{4.11}$$

$$m_y = \cos(y, Y) = \cos\alpha = \frac{X_j - X_i}{l_e} \tag{4.12}$$

The coordinate transformation in the "X–Y" plane does not affect the rotational DOF, as its direction is in the "z" direction (normal to the x–y plane), which still

remains the same as the “Z” direction in the global coordinate system. The length of the element, “l_e” can be calculated by Equation 4.13.

$$l_e = \sqrt{\left(X_j - X_i\right)^2 + \left(Y_j - Y_i\right)^2} \tag{4.13}$$

Equation 4.7 can be easily verified, as it simply says that at node “i”, "U_1" equals the summation of all the projections of “D_{3i-2}” and “D_{3i-1}”on to the local “x” axis, and “v_1” equals the summation of all the projections of “D_{3i-2}” and “D_{3i-1}” on to the local “y” axis. The same can be said at node “j”. The matrix “T” for a frame element transforms a “6 × 6” matrix into another “6 × 6” matrix. Using the transformation matrix, “T”, the matrices for the frame element in the global coordinate system is found.

$$K_e = T^T k_e T \tag{4.14}$$

$$M_e = T^T m_e T \tag{4.15}$$

$$F_e = T^T f_e \tag{4.16}$$

CHAPTER 5

FINITE ELEMENT ANALYSIS OF THREE LINKS FLEXIBLE PLANER MANIPULATOR

5.1. Introduction

For the finite element analysis of three link flexible planer manipulator, the static analysis is done assumed the links are moving slow enough. The calculation delivered is not time dependent and computed just after the time when the motors at joints stop and the system have enough time to be a steady state. The general equation for stiffness given in Equation 5.1 is applied for the each link's frame element. The analysis is calculated for the first path and second path of each position in Equation 5.1

$$\{F\} = [k_e]\{x\} \tag{5.1}$$

The force that causes the deflection in frame element is given as "$\{F\}$",

The stiffness of each frame element is given as "$[k_e]$" matrix,

The displacement of each frame element is given as "$\{x\}$"

5.2. Finite Element Model

The elastic displacements because of the applied force and gravity cause the total tip displacements. To calculate the displacements and overcome reaching the tip wrong point, that's needed to apply extra torque value for each joint of the manipulator. With finite element method each manipulator link is divided to 3 unit element as it shown in Figure 5.1 and Figure 5.3 consecutively for first and second solutions. These elements are connected to each other at their nodes. The element numbers are shown "e_i" and the nodes that connects the elements are shown "n_i".The mass of each link is assumed "M" and shared at the tips of the each link as "M/2". The mass distribution of the three links manipulator is shown in Figure 5.2 and Figure 5.4.

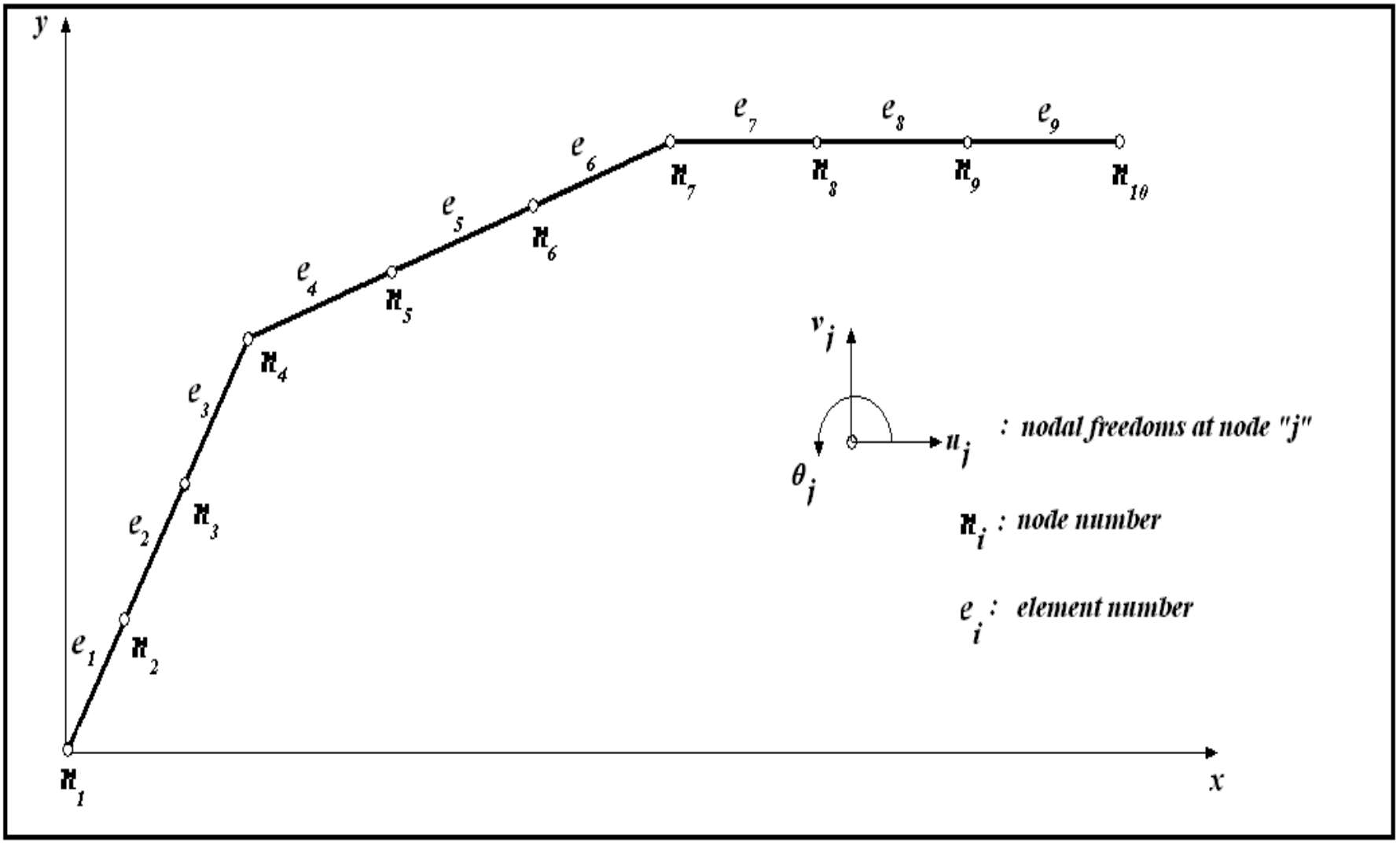

Figure 5.1. Three link manipulator's nodes for the first solution

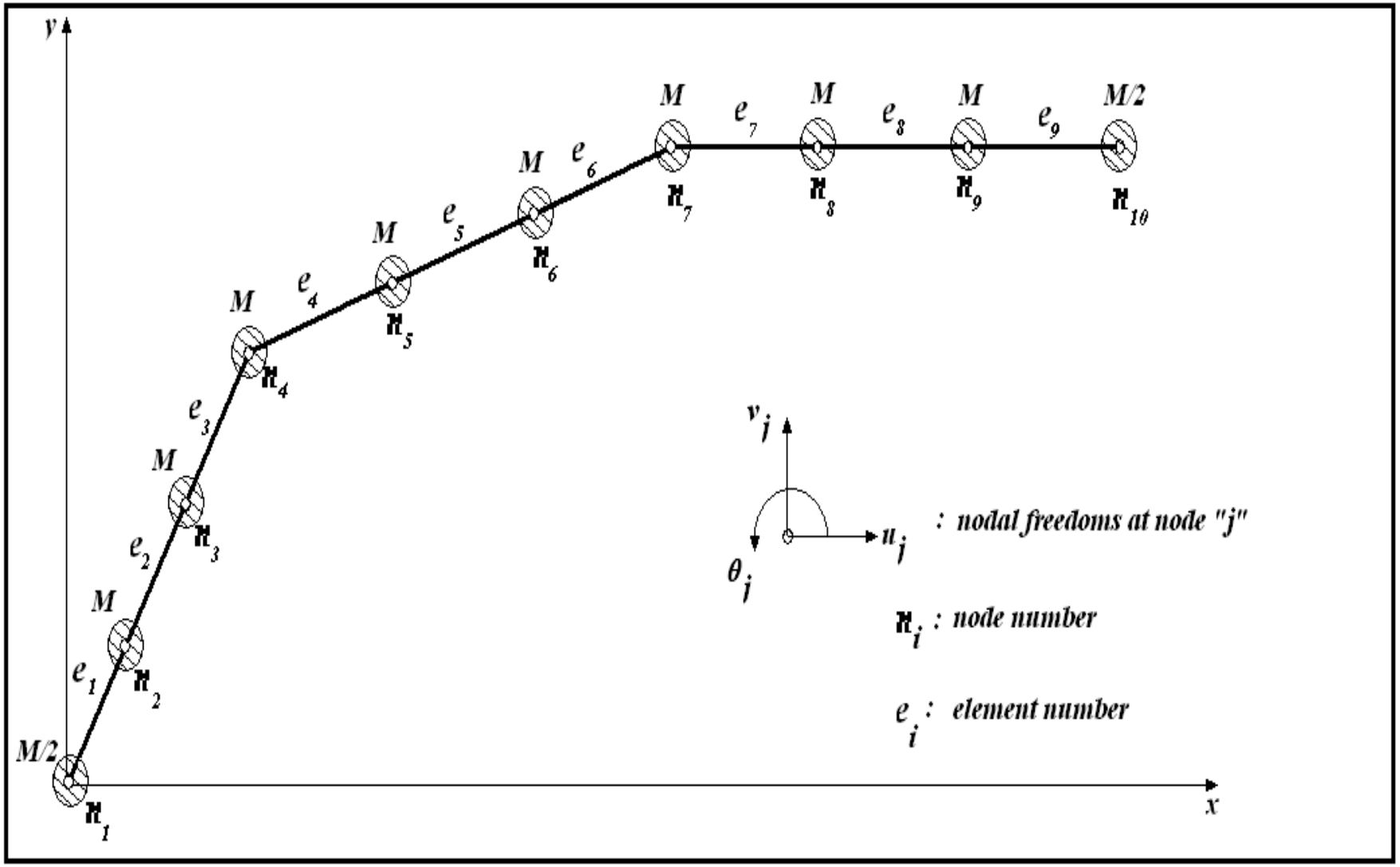

Figure 5.2. Mass distributions of three link manipulator for the first solution

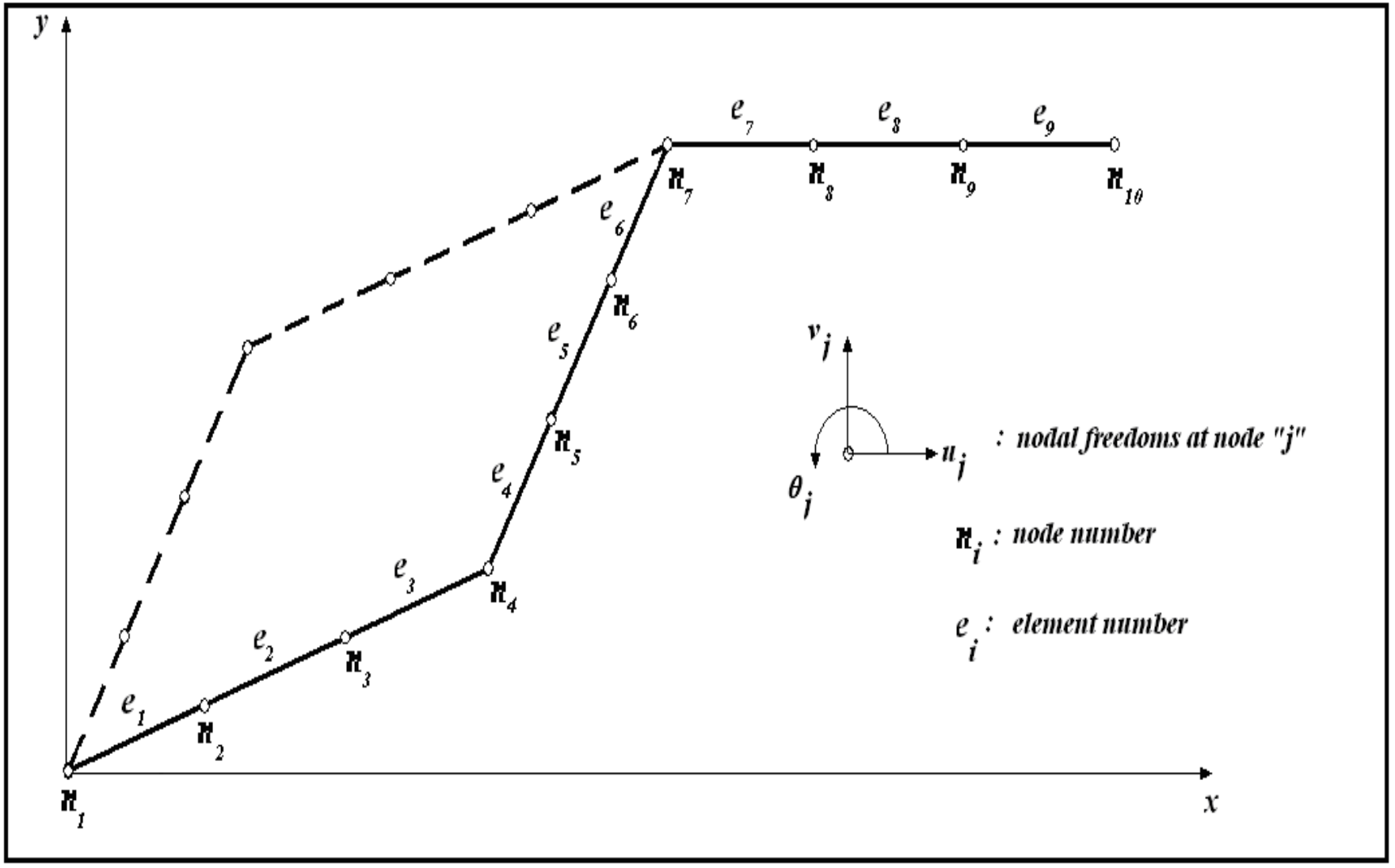

Figure 5.3. Three link manipulator's nodes for the second solution

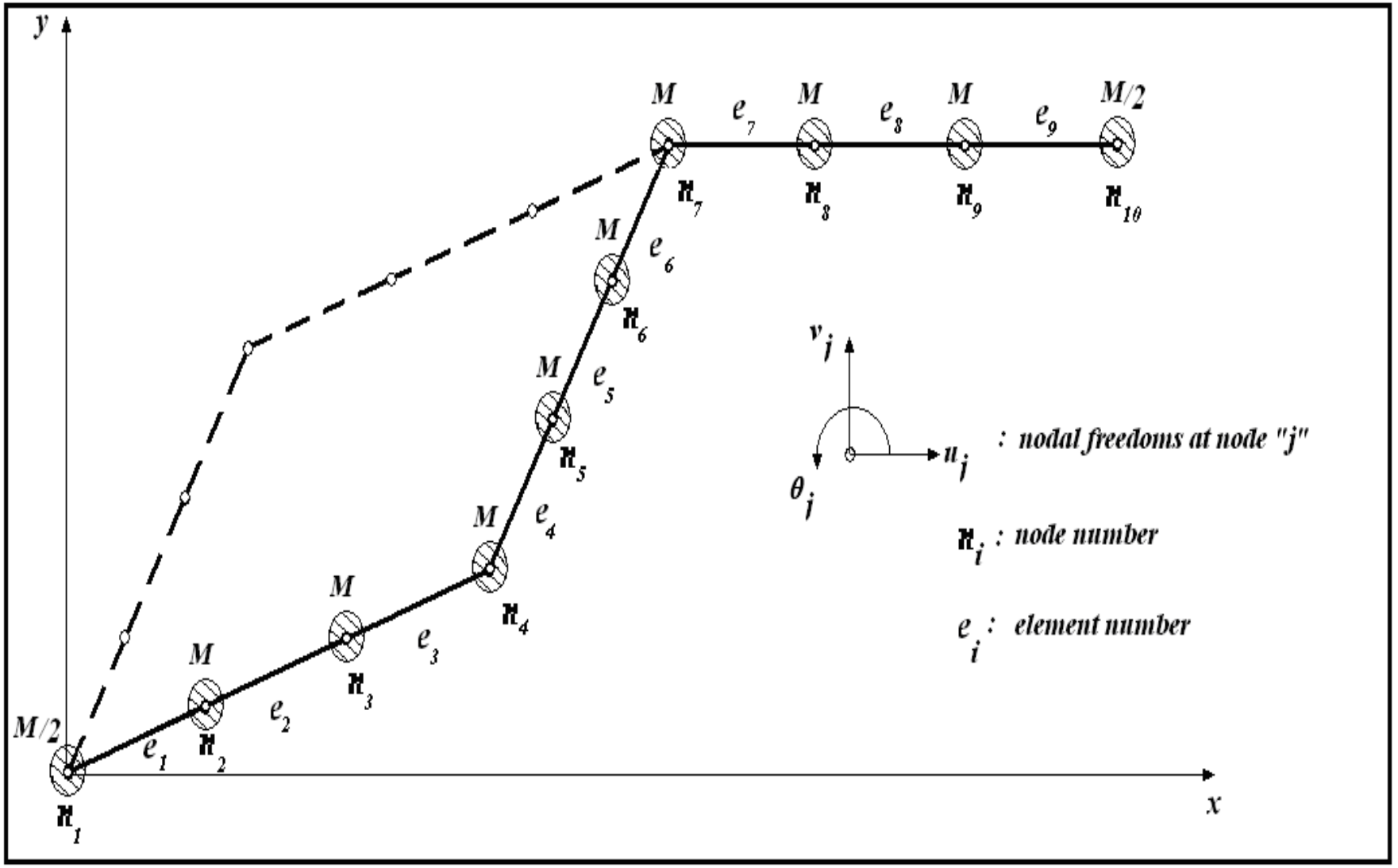

Figure 5.4.Mass distributions of three link manipulator for the second solution

CHAPTER 6

NUMERICAL EXAMPLE

6.1. Defining Manipulator

In this thesis, three link flexible planer manipulator is designed to operate as a library robot. It is assumed that the link three is always in horizontal direction and moves through the shelves, spaced "150" mm in vertical direction as shown in Figure 2.1. The manipulator carries a book at the tip of link three, considered "30" N weight itself. The manipulator has one constrain to the ground at the bottom face of the link one. The calculation delivered is not time dependent and computed just after the time when the motors stop and the system have enough time to be a steady state.

In the design, it is assumed that the manipulators are made of two different material and three different cross-section which their properties and result given below. The safety factor of each design for the maximum pure bending is kept same as approximately "4". Also the following parameters are applied.

In the first example, the ratio of "h/b" is equal to "3" with material 1100-H12 Aluminum and the displacements of the tip point are found. In the second example, the ratio of "h/b" is chosen as the same with first example according to get the same safety factor with material C1030 normalized steel. In the third example, "b" is chosen as the same with first example and "h" is calculated using the same safety factor of first example.

The geometrical and material properties of the manipulator designed with 1100-H12 Aluminum for the first example and C1030 normalized steel for the second and third example are expressed below;

In the first example, manipulator with 1100-H12 aluminum link;

Elasticity Module: $E=70\ GPa$

Density; $\rho = 2710 kg/m^3$

Link Lengths; $l_1 = l_2 = l_3 = 600 mm$

The cross-section dimensions: *b (width)= 10 mm, h(height)= 30 mm*

In the second and third examples, manipulator with C1030 normalized steel link:

Elasticity Module: *E=200 GPa*

Density; $\rho = 7850 kg/m^3$

Link Lengths; $l_1 = l_2 = l_3 = 600 mm$

The cross-section dimensions of second example manipulator link:

b (width)= 6.8mm, h(height)= 20.4mm.

The cross-section dimensions of third example manipulator link:

b (width)= 10mm, h(height)= 18mm.

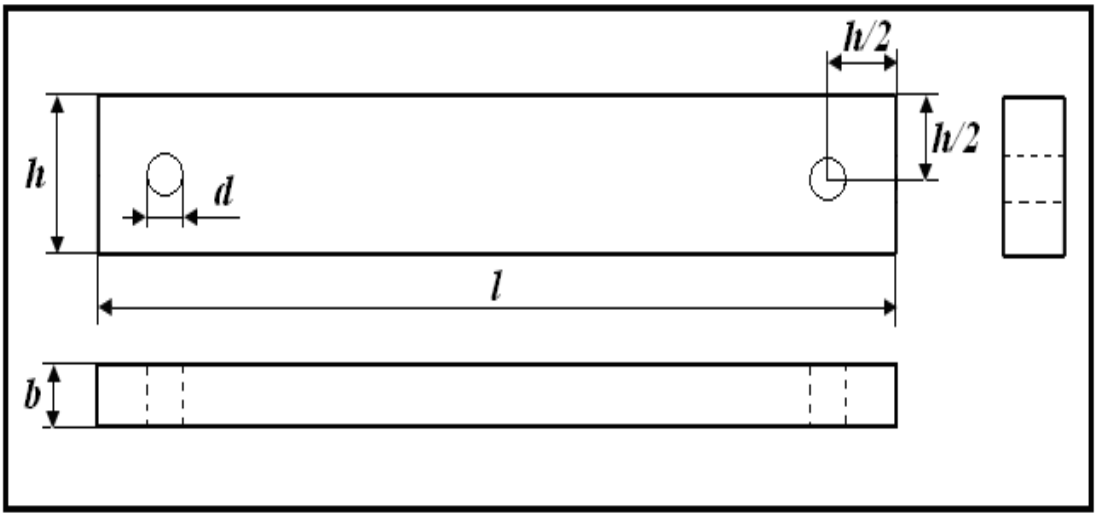

Figure 6.1. Technical drawing of the link

All the links of the manipulator have the same dimensions and cross sections. The technical drawing of one link is shown in Figure 6.1.

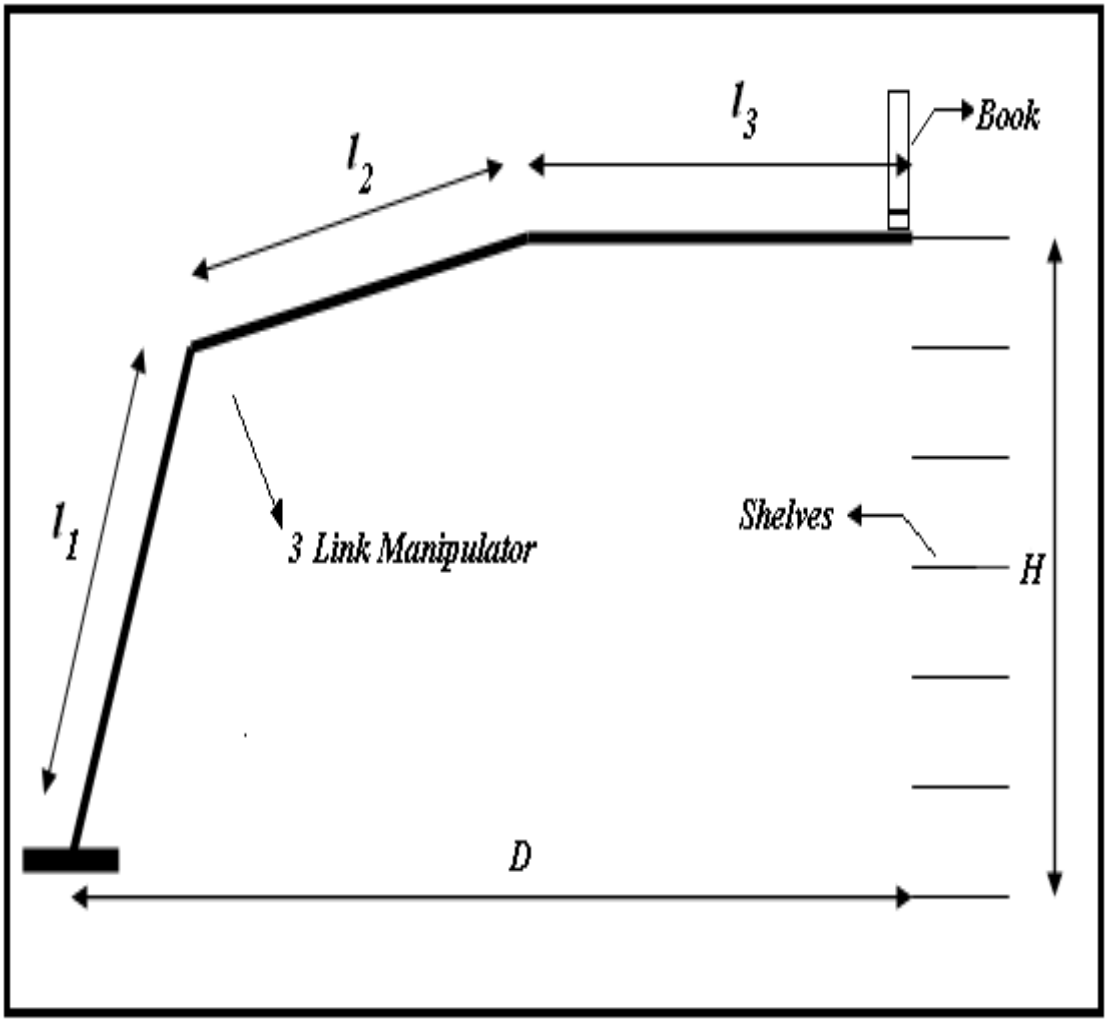

Figure 6.2. The path of three link flexible planer manipulator

The path of three link flexible planer manipulator is shown in Figure 6.2. The other numerical values are as follows;

The mass of the book;

$M_{Book} = 3{,}05kg$

Horizontal distance from base of the manipulator to shelves;

D=1100mm

Vertical distance from ground to top shelf;

H=900mm

6.2. Inverse Kinematic Analysis Results for Flexible Manipulator

The first and second solutions of inverse kinematic analysis are given in Table 6.1 and Table 6.2.

Table 6.1. The first solution of inverse kinematic analysis

Position Number	Desired Position of the Tip(x, y) (mm)	$\theta_1(^\circ)$	$\theta_2(^\circ)$	$\theta_3(^\circ)$
1	(1100,900)	91,86	30,04	0
2	(1100,750)	97,62	15,00	0
3	(1100,600)	99,59	0,80	0
4	(1100,450)	97,89	-13,92	0
5	(1100,300)	91,86	-29,96	0
6	(1100,150)	80,91	-47,52	0
7	(1100,000)	65,38	-65,38	0

Table 6.2. The Second solution of inverse kinematic analysis

Position Number	Desired (x, y) Position of the Tip(mm)	$\theta_1(^\circ)$	$\theta_2(^\circ)$	$\theta_3(^\circ)$
1	(1100,900)	30,04	91,86	0
2	(1100,750)	15,00	97,62	0
3	(1100,600)	0,80	99,59	0
4	(1100,450)	-13,92	97,89	0
5	(1100,300)	-29,96	91,89	0
6	(1100,150)	-47,52	80,91	0
7	(1100,000)	-65,38	65,38	0

6.3. Example 1

With developed Matlab Program, displacements of tip of the manipulator with 1100-H12 aluminum links are calculated. The results are shown in Table 6.3 and Table6.4.

Table 6.3.Displacements of tip point for the first solution of joint angles (1100-H12 aluminum manipulator, *b=10mm, h=30mm)*

Position Number	Desired Position of Tip Point(x, y) (mm)	$\theta_1(^\circ)$	$\theta_2(^\circ)$	$\theta_3(^\circ)$	Displacements of Tip Point ($\Delta x, \Delta y$)(mm)
1	(1100,900)	91,86	30,04	0	(6,29 ; -9,56)
2	(1100,750)	97,62	15,00	0	(5,14 ; -9,74)
3	(1100,600)	99,59	0,80	0	(3,94 ; -9,80)
4	(1100,450)	97,89	-13,92	0	(2,71 ; -9,75)
5	(1100,300)	91,86	-29,96	0	(1,49 ; -9,57)
6	(1100,150)	80,91	-47,52	0	(0,30 ; -9,23)
7	(1100,000)	65,38	-65,38	0	(-0,77 ; -8,80)

Table 6.4.Displacements of tip point for the second solution of joint angles (1100-H12 aluminum manipulator, *b=10mm, h=30mm)*

Position Number	Desired Position of Tip Point(x, y) (mm)	$\theta_1(^\circ)$	$\theta_2(^\circ)$	$\theta_3(^\circ)$	Displacements of Tip Point ($\Delta x, \Delta y$)(mm)
1	(1100,900)	30,04	91,86	0	(6,23 ; -8,11)
2	(1100,750)	15,00	97,62	0	(5,26 ; -7,96)
3	(1100,600)	0,80	99,59	0	(4,34 ; -7,91)
4	(1100,450)	-13,92	97,89	0	(3,45 ; -7,96)
5	(1100,300)	-29,96	91,89	0	(2,59 ; -8,11)
6	(1100,150)	-47,52	80,91	0	(1,71 ; -8,39)
7	(1100,000)	-65,38	65,38	0	(0,77 ; -8,80)

6.4. Example 2

With developed Matlab Program, displacements of tip of the manipulator with AISI-C1030 normalized steel links are calculated .The results are shown in Table 6.5 and Table 6.6.

Table 6.5. Displacements of tip point for the first solution of joint angles (AISI-C1030 normalized steel manipulator *b=6.8mm, h=20.4mm)*

Position Number	Desired Position of Tip Point(x, y) (mm)	$\theta_1(^\circ)$	$\theta_2(^\circ)$	$\theta_3(^\circ)$	Displacements of Tip Point ($\Delta x, \Delta y$)(mm)
1	(1100,900)	91,86	30,04	0	(10,81 ; -16,41)
2	(1100,750)	97,62	15,00	0	(8,82 ; -16,72)
3	(1100,600)	99,59	0,80	0	(6,66 ; -16,82)
4	(1100,450)	97,89	-13,92	0	(4,66 ; -16,73)
5	(1100,300)	91,86	-29,96	0	(2,56 ; -16,42)
6	(1100,150)	80,91	-47,52	0	(0,53 ; -15,85)
7	(1100,000)	65,38	-65,38	0	(-1,31 ; -15,12)

Table 6.6. Displacements of tip point for the second solution of joint angles (AISI-C1030 normalized steel manipulator *b=6.8mm, h=20.4mm)*

Position Number	Desired Position of Tip Point(x, y) (mm)	$\theta_1(^\circ)$	$\theta_2(^\circ)$	$\theta_3(^\circ)$	Displacements of Tip Point ($\Delta x, \Delta y$)(mm)
1	(1100,900)	30,04	91,86	0	(10,73 ; -13,95)
2	(1100,750)	15,00	97,62	0	(9,73 ; -13,70)
3	(1100,600)	0,80	99,59	0	(7,47 ; -13,62)
4	(1100,450)	-13,92	97,89	0	(5,94 ; -13,69)
5	(1100,300)	-29,96	91,89	0	(4,45 ; -13,95)
6	(1100,150)	-47,52	80,91	0	(2,94 ; -14,43)
7	(1100,000)	-65,38	65,38	0	(1,31 ; -15,12)

6.5. Example 3

With developed Matlab Program, displacements of tip of the manipulator with AISI-C1030 normalized steel link is calculated .The results are shown in Table 6.7 and Table 6.8.

Table 6.7 Displacements of tip point for the first solution of joint angles (AISI-C1030 normalized steel manipulator *b=10mm, h=18mm)*

Position Number	Desired Position of Tip Point(x, y) (mm)	$\theta_1(^\circ)$	$\theta_2(^\circ)$	$\theta_3(^\circ)$	Displacements of Tip Point ($\Delta x, \Delta y$)(mm)
1	(1100,900)	91,86	30,04	0	(11,30 ; -17,13)
2	(1100,750)	97,62	15,00	0	(9,22 ; -17,44)
3	(1100,600)	99,59	0,80	0	(7,07 ; -17,55)
4	(1100,450)	97,89	-13,92	0	(4,87 ; -17,46)
5	(1100,300)	91,86	-29,96	0	(2,67 ; -17,14)
6	(1100,150)	80,91	-47,52	0	(0,56 ; -16,55)
7	(1100,000)	65,38	-65,38	0	(-1,37 ; -15,80)

Table 6.8 Displacements of tip point for the second solution of joint angles (AISI-C1030 normalized steel manipulator *b=10mm, h=18mm)*

Position Number	Desired Position of Tip Point(x, y) (mm)	$\theta_1(^\circ)$	$\theta_2(^\circ)$	$\theta_3(^\circ)$	Displacements of Tip Point ($\Delta x, \Delta y$)(mm)
1	(1100,900)	30,04	91,86	0	(11,23 ; -14,59)
2	(1100,750)	15,00	97,62	0	(9,49 ; -14,34)
3	(1100,600)	0,80	99,59	0	(7,82 ; -14,26)
4	(1100,450)	-13,92	97,89	0	(-6,22 ; -14,33)
5	(1100,300)	-29,96	91,89	0	(4,65 ; -14,60)
6	(1100,150)	-47,52	80,91	0	(3,07 ; -15,09)
7	(1100,000)	-65,38	65,38	0	(1,37 ; -15,80)

6.6. Discussion of the Results

The results show that the absolute displacements of tip of the manipulator is in "x" direction range between "0.3"mm to "6.23"mm for the 1100-H12 aluminum manipulator with *(b=10mm, h=30mm)* , 0.53mm to 10.81mm for the AISI-C1030 normalized steel manipulator with *(b=6.8mm, h=20.4mm)* and "0.56"mm to "11.30" mm for the AISI-C1030 normalized steel manipulator with *(b=10mm, h=18mm).*

Also the absolute displacements in "y" direction range between "7.91"mm to "9.80"mm for the 1100-H12 aluminum manipulator with *(b=10mm, h=30mm)* , "13.62"mm to "16.82" mm for the AISI-C1030 normalized steel manipulator with *(b=6.8mm, h=20.4mm)* and "14.26"mm to "17.55"mm for the AISI-C1030 normalized steel manipulator with *(b=10mm, h=18mm).*

From these results, it can be seen that the lighter material with higher cross-section area has the minimum displacement range. Example 1 one has the minimum displacements in all three example design. Also, between second and third example design in which the same material is used, lower displacement is seen at Example 2. As a result, so many factors have to be included and optimized for the best design such as materials, shape of the links and dimensions.

CHAPTER 7

CONCLUSION

In this thesis, the path generation analysis of three links planer flexible manipulator is investigated and displacements of the tip of the manipulator are found with the developed finite element program in Matlab. Since the manipulator has no inertia forces static analysis to get tip of the displacement adequate. As a future work, this analysis should be done in time domain and vibrations should not be neglected, to get more accurate results.

REFERENCES

Book, W.J. 1984. Recursive Lagrangian Dynamics of Flexible Manipulator Arms. *The International Journal of Robotic Research* 3(3): 87-101.

De Luca, A. and B.Siciliano. 1991. Closed-form Dynamic Model of Planar Multilink Lightweight Robots**.** *Systems, Man and Cybernetics, IEEE Transactions on* 21(4): 826-839.

Yuan, B.S. and W.J. Book and J. D. Huggins. 1994. Dynamics of Flexible Manipulator Arms: Alternative Derivation, Verification, and Characteristics for *Control Journal of dynamic systems, measurement, and control* l15(3): 1-11.

Canudas, C and B. Siciliano and G. Bastin. 1996. Theory of Robot Control. *Springer-Verla*g: 219-265.

De Luca, A. and B. Siciliano. 1993. Regulation of Flexible Arms Under Gravity. *Robotics and Automation, IEEE Transactions* 9(4)**:** 463-467.

De Luca, A. and S. Panzieri. 1994 An Iterative Scheme for Learning Gravity Compensation in Flexible Robot Arms. *Automatica* 30(6): 993-1002.

Dawson, D.M. and Z. Qu and J. Carroll.1991. Robust Tracking of Rigid Link Flexible Joint Electrically Driven robots. *International Journal of Control* 56(5): 991-1006.

Craig, J.J. 1989. Introduction to Robotics Mechanics and Control Second Edition. *Addison-Wesley*: 113-144.

Liu, G.R. 1993.The Finite Element Method: A Practical Course. *Butterworth*: 108-114.